

# An analysis of the “Fast” noise measurements of the dynamic VVER processes<sup>\*</sup>

Gennady V. Arkadov<sup>1</sup>, Vladimir I. Pavelko<sup>2</sup>, Mikhail T. Slepov<sup>3</sup>

1 Non-Profit Partnership for Promoting the Development of System Engineering “Rise”, 5/12 bld. 3 Zeleniy pr., 111141 Moscow, Russia

2 Scientific and Technical Center Diaprom JSC, 6 Koroleva Str., 6249031 Obninsk, Kaluga Reg., Russia

3 Branch of Concern Rosenergoatom JSC Novovoronezh NPP, 1 Industrial zone Yuzhnaya, 396072 Novovoronezh, Voronezh Reg., Russia

Corresponding author: Mikhail T. Slepov (slepovmt@nvnpp1.rosenergoatom.ru)

**Academic editor:** Georgy Tikhomirov ♦ **Received** 14 August 2023 ♦ **Accepted** 21 November 2023 ♦ **Published** 29 March 2024

**Citation:** Arkadov GV, Pavelko VI, Slepov MT (2024) An analysis of the “Fast” noise measurements of the dynamic VVER processes. Nuclear Energy and Technology 10(1): 63–71. <https://doi.org/10.3897/nucet.10.123398>

## Abstract

Studies of maneuverable modes of VVER to confirm the possibility of participation of nuclear power plants in the mode of daily carrying capacity have been conducted for quite a long time. Tests at various nuclear power plants with VVER-1000 (Zaporizhzhia NPP in 1998, Khmelnytsky NPP in 2005, Tianwan NPP in 2007) have shown the practical possibility of NPP participation in the daily schedule of carrying capacity, however, the commissioning of nuclear power plants with VVER-1200 requires similar work on all new units with VVER-1200: NVAES-2, LNPP-2 Belarusian NPP. The article presents some aspects of the use of noise control methods for analyzing the condition of equipment and the core.

Since the emergence of the technology of noise analysis of signals from VVER reactor installations, researchers have formulated several criteria for obtaining results of appropriate quality. The fundamental requirement for conducting noise experiments was the registration of data in stationary modes of operation of power units, since any non-stationarity made significant changes in spectral estimates, which ultimately complicated the work and “distorted” the results obtained. This requirement was included in the operating instructions of various diagnostic systems using noise signal analysis methods (the SUS system, manufactured by Siemens). For a long period of time, the current situation suited both developers of various diagnostic systems and NPP personnel operating them at power units. On the one hand, this was due to the imperfection of the technical means used (low speed of analog-to-digital converters, limited storage capacity, bulky equipment, etc.), on the other hand, the use of domestic NPP power units only in the base load mode without tracking daily power fluctuations in the power system.

The standard archives of the upper block level system, the in-reactor control system and additionally produced multi-channel “fast” measurements with a frequency of 1 kHz for the analysis of maneuverable mode 95-55-95% of the VVER-1200 reactor plant were analyzed. Global disturbances of the core have been detected after one step of the regulatory body of the control and protection system, which attenuates within one second if the next step of the control and protection system has not occurred during this time. Such fast neutron processes can be controlled only by neutron-noise measurements with an upper frequency of at least 20 Hz.

## Keywords

VVER-1200, xenon oscillations, offset, boron regulation, steam phase, neutron noise, spectrum, acoustic standing waves

\* Russian text published: Izvestiya vuzov. Yadernaya Energetika (ISSN 0204-3327), 2023, n. 4, pp. 19–36.

## Introduction

Since the emergence of the technology for noise analysis of signals from VVER reactor plants, different groups of researchers have formulated, independently of each other, a number of criteria for recording information to obtain results of an appropriate quality for subsequent analysis. The fundamental requirement with respect to noise experiments was recording of data in steady-state operating modes of power units, since any unsteadiness caused major changes to spectral estimates, which complicated, in the long run, the experiments and invalidated the results obtained. This requirement was made part of instructions for operating different diagnostic systems using noise techniques for analyzing signals (the SÜS<sup>1</sup> system from Siemens). For a long time, this situation suited both the developers of diagnostic systems and the NPP personnel responsible for their operation at power units. On the one hand, this was explained by imperfect equipment used (low speed of analog-to-digital converters, limited data storage volumes, cumbersome hardware, etc.), while, on the other hand, by the fact that Russian-designed NPP units were used only in the base loading mode without tracking daily power fluctuations in the power grid.

The commissioning of VVER-1200 units expected, as initially designed, to take part in daily power regulation, led to the need to arrange for and conduct noise measurements in the process of transients. The paper presents selected results from noise investigations of maneuvering modes for the VVER-1200 reactor of the Novovoronezh NPP-2's unit 1 conducted in September 2022 in accordance with the developed work program. The work program describes in a step-by-step manner the actions to be taken by the NPP personnel for ten consecutive maneuvering days based on different implementation strategies. Under consideration here is the tenth day with the so-called rigid power regulation. The work program, as the authors believe, contains a questionable closing statement: “No dedicated methodology is required to process the results. The results are processed based on tables and diagrams from the UULS, ICIS and CPS power equipment system archives”. Using the same archives and having additionally performed multichannel “fast” measurements with a frequency of 1 kHz, we shall analyze this maneuvering mode.

## Brief historical background and chronology of events

VVER maneuvering modes have been studied, both computationally and theoretically and via full-scale experiments, over a long period of time (Ignatenko and Pytkin 1985; Aver'yanova et al. 2002, 2007, 2008, 2017, 2018; Tereshonok et al. 2003; Averyanova et al. 2005, 2010, 2013; Aver'yanova and Filimonov 2009; Averyanova et al. 2012; Glushenkov 2015; Vygovsky et al. 2018; Filimonov et al. 2020, 2022; Povarov et al. 2021).

Specifically, full-scale VVER-1000 testing was undertaken at the Zaporizhzhia NPP in 1998 (Averyanova et al. 2005), at the Khmelnytskyi NPP in 2005 (Averyanova et al. 2010), and at the Tianwan NPP in 2007 (Averyanova et al. 2012). It follows from the chronologically listed references that power maneuvering is still of interest, this being confirmed by maneuvering tests having been conducted at all new units with VVER-1200s (Novovoronezh NPP-2, Leningrad NPP-2, Belarusian NPP) since the initial operating cycle (Averyanova et al. 2013; Glushenkov 2015; Aver'yanova et al. 2017, 2018; Vygovsky et al. 2018; Filimonov et al. 2020). Different strategies of maneuvering modes have therefore evolved in the course of searching for the best possible option. After each stage of testing, upgrades were proposed for the existing design equipment of reactor plants, as well as ways to automate the maneuvering mode following.

Normally, tests were conducted for not more than 10 days. A full-scale daily maneuvering mode suggests continuous operation for not less than two hundred effective days (Povarov et al. 2021).

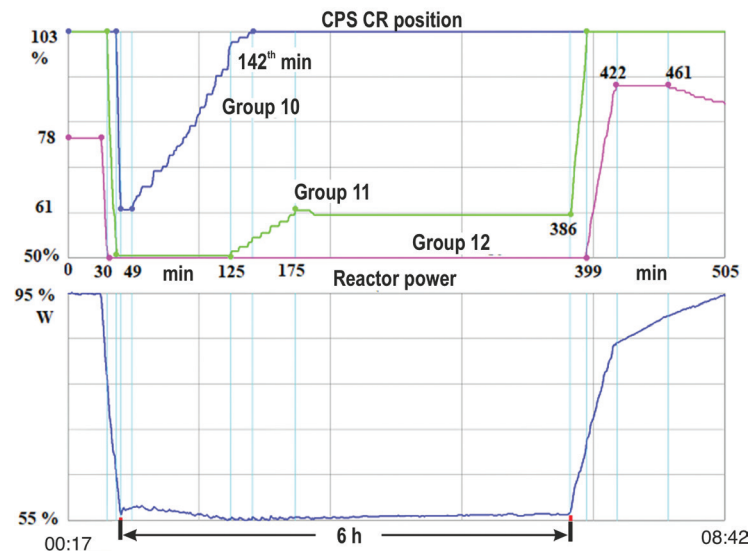
The traditional name for the daily maneuvering mode (100%–50%–100%) is historical and does not reflect the reality nowadays. After numerous calculations and experiments, the upper power level in the mode name was changed for 96% due to the need for maintaining reliable operation of the turbine generator (TG). The lower power level varies in a range of 45% to 75%.

Fig. 1 presents the reactor power as a function of time. The time interval is 505 minutes (00:17 – 08:42). The time markers (in minutes) in the diagram show the points when typical changes in the CPS control rod (CR) positions take place for groups 10, 11 and 12.

Thirty minutes after the recording starts from the steady-state power condition of 95%, the CPS CR control groups move, one after another, to the planned lower extreme positions. First, group 12 moves from the 78% position to the 50% position, and then group 11 moves from the 103% position (the upper limit switch (ULS)) to the 50% position, followed by group 10 moving from the 103% position (ULS) to the 62% position.

The control rod groups move at the maximum permissible speed resulting in a power reduction rate of 3% per minute, which corresponds to a TG power cutback rate of 36 MW per minute. Thus, it takes 15 minutes for all three groups to occupy their lowest planned position. The reactor power drops from 95% to 55% in such a short time.

Apart from the CPS CR group positions and the reactor power, the smallest possible values are assumed by the axial offset ( $-47\%$ ), which is much below the recommended offset values, and by the core inlet coolant temperature of  $291\text{ }^{\circ}\text{C}$  ( $T_{in}=291\text{ }^{\circ}\text{C}$ ).  $T_{in}$  increases then slightly as a result of the temperature reactivity effect, this being possibly explained by overshooting. The blow-down water flow rate and the boric acid concentration change within this short period of time, i.e. the minimum planned power level of 55% is achieved by two key reactivity impacts (movement of three CPS CR groups and water exchange).



**Figure 1.** Change in the position of control rod groups (upper diagram) and the reactor power variation (lower diagram) in the course of maneuvering mode.

The process of transition from 95% to 55% is a very high-speed transient that will further define the negative aspects of power maneuvering. Such a fast and large amplitude change in the reactor power also causes major axial xenon oscillations (XOs) in the downward phase (i.e., those aimed at reducing the reactor power).

The second test stage (keeping power at a level of 55% for six hours) starts so and is accompanied further by major XOs. Three CPS CR groups, being at their minimum predicted positions, lead to the core power density field being highly heterogeneous, which reduces the fuel burnup. This is confirmed by the minimum value of the axial offset with a level of  $-47\%$ , i.e. the smallest possible power of 55% is generated largely by the lower half of the core.

As early as 19 minutes after the test begins, the CPS CR group 10 starts to travel in the opposite direction (upward), introducing positive reactivity and compensating so for the downward XO trend (Averyanova et al. 2010; Aver'yanova et al. 2017; Filimonov et al. 2022; Dolgoplov and Mezentsev 2022). In just 100 minutes, the CPS CR group 10 traveled back from the ULS position, after having reached an insertion depth of 62%, to the initial ULS position with a large number of traveling steps done solely to suppress the downward XO phase. At the same time, the reactor power is kept for six hours (nighttime period), with a high accuracy, at a constant level of 55% not only by the CPS CRs but also via self-regulation on the secondary circuit side. Power maintenance with a high accuracy is the second negative factor of this maneuvering mode. At this point, water exchange is possible as another reactivity factor if self-regulation on the TG side reaches the permissible limits by keeping the steam pressure in the main steam header (MSH) constant. Self-regulation by keeping the MSH pressure in a narrow “corridor” is the key property of maneuvering referred to as rigid power regulation. An increase in the water exchange volume, as compared with the base steady-state mode of reactor

operation, is a negative factor in terms of the maneuvering mode implementation.

Group 11 starts to move upward at the 125<sup>th</sup> minute, that is, there is a time interval when two groups (10 and 11) are moving upward, and group 12 does not change its lower position. An increase in the number of the CPS CR steps, compared with the base steady-state mode of reactor operation, is also a negative factor for the maneuvering mode implementation. The upward movement of groups 10 and 11 increases the offset monotonously from  $-47\%$  to  $-34\%$  shifting so insignificantly power generation into the upper half of the core. The core is in a continued transient state, which brings to an end at a growing rate the lifetime of fuel elements, the CPS CRs, the group and individual control system, and all other reactivity controls. In the course of this period, self-regulation (Fig. 1) is exercised in relatively frequent acts. After groups 10 and 11 reach steady states, self-regulation changes its nature (Fig. 1).

With two groups of rods being in motion, the steam pressure in the steam generator header has the form of a noisy constant as the parameter that characterizes self-regulation on the turbine side. At the 175<sup>th</sup> minute, after two groups (10 and 11) reach their steady states (at the ULS position for group 10, and at the 61% level for group 11), the axial offset goes down again to  $-40\%$  in accordance with the linear dependence.

The change in the primary coolant rate as a function of reactor power is a density effect: the coolant density (and the mass flow rate) increases as the coolant temperature decreases. However, in the time interval when power is kept constant at a level of 55%, the coolant flow rate decreases monotonously through the heat exchange loops (by 2%). With power density being unsteady, the local thermal-hydraulic characteristics of the core portions change causing so a change in the amount of the coolant flowing across the fuel assemblies and in the coolant crossflows between neighboring fuel assemblies (as estimated by the authors, using noise

analysis techniques leads to the value of the coolant cross-flows between neighboring fuel assemblies reaching 4% of the total cross-sectional coolant flow). The implementation of this maneuvering mode causes an uncertainty of heat removal or the fuel assembly (FA) rating. In addition, the integral hydraulic resistance of the entire core also changes to a certain extent changing so the total pressure drop across the core and the total coolant flow in the primary circuit.

In the course of this time, the core inlet coolant temperature,  $T_{in}$ , increases. This reactivity margin is used then in the event the reactor power increases from 55% to 95%, including as well at the expense of the negative temperature coefficient of reactivity.

After six hours of keeping power at a level of 55%, the 55%-95% transient takes place as the CPS CR groups 11 and 12 move upwards. There is also an increase in the blowdown water flow rate and a decrease in the boric acid concentration, which remained practically unchanged at the 55% power level. As a result, power increases to 87% in a linear fashion at a rate three times less than the power reduction rate at the initial stage (95%-55%). At the 399<sup>th</sup> minute, group 11 reaches its ULS, and group 12 stops moving upward after 422 minutes while the power increase follows further the upward phase of XOs, which begin to be suppressed again by the movement of the CPS CR group 12 which is, however, downward this time.

The axial offset enters again the recommended range and reaches +2%. Therefore, this is rather a complex maneuvering mode, which involves all control reactivity actions (CRAs), and the CPS CRs travel upward and downward not only for changing power but also to keep power at a constant level as a result of the XO suppression.

## Neutron field in the process of the cps cr movement

Standard control rod movements down into the core (CPS CR groups 10, 11 and 12) in the 95%-55% transient are accompanied by downward bursts of the core neutron power, and, as the control rod move downward, the burst amplitude decreases monotonously (Fig. 2). As group 12 travels upward in the 55%-95% transient, there is also a downward neutron power burst observed (Fig. 3). This upward movement of group 12 leads to an increase in the burst amplitude, and there is also an upward trend in the root-mean-square (RMS) value of the neutron background noise. Such neutron flux dynamics,  $n(t)$ , is explained by the different rate of its change,  $n(t)/dt$ , depending on the insertion of negative reactivity (downward movement of the CPS CRs) and positive reactivity (upward movement of the CPS CRs).

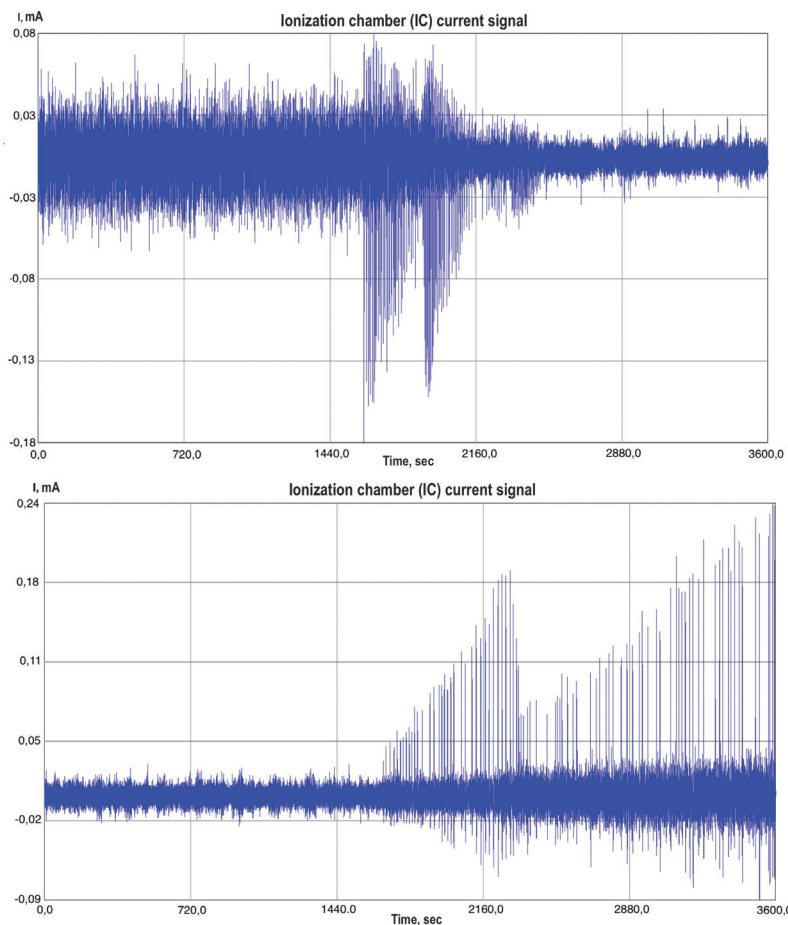


**Figure 2.** Fragments of neutron power from IC signals at the beginning of the power reduction due to downward movement of the CPS CRs in the 95%-55% transient (upper diagram) and at the beginning of the power increase in the 55%-95% transient due to the upward movement of group 12.

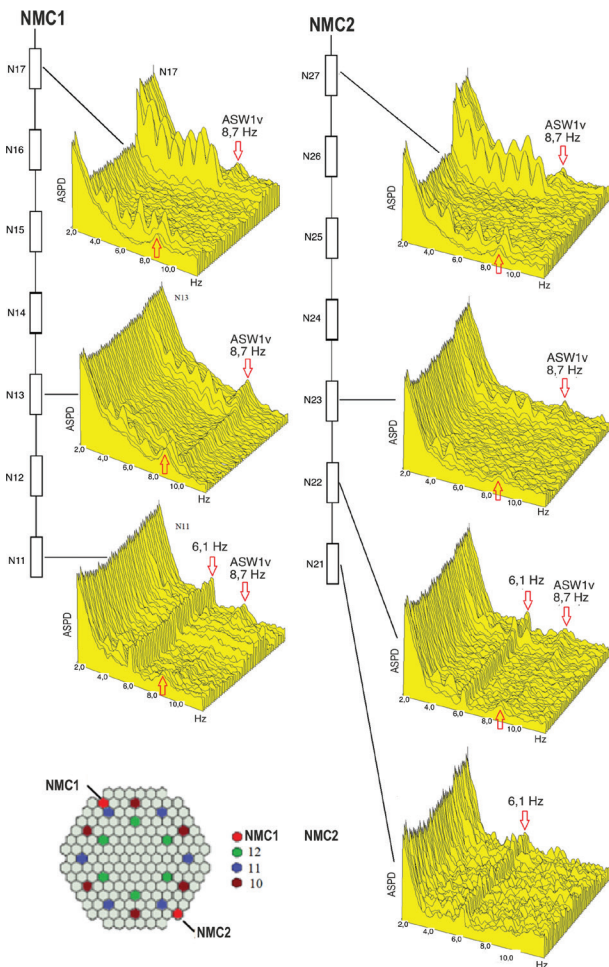


**Figure 3.** Autospectral power density (ASPD) of the NMC1 (left column) and NMC2 (right column) direct-charge detector (DCD) signals. The arrows show two resonant features: ASW1v (8.7 Hz) and the vibration resonance at 6.1 Hz.

Relative to the level of the stationary neutron noise, a single step of any CPS CR group causes a much larger amplitude of the neutron noise burst. If one compares the stationary NN RMS and the NN burst amplitude as a result of one CPS CR step, a difference of three to five times will be obtained. After a single CPS CR step, the whole of the core is exposed to a practically instantaneous major amplitude effect, which fades away within one second if no further CPS CR step takes place during this time. Such rapid neutron processes can only be detected by neutron noise measurements up to the upper frequency of not less than 20 Hz.

Right after reaching the 55% power level, there follows a short time interval during which there are no CRAs and, specifically, there is no CPS CR movement. At this point, NN is a nearly steady-state process with the RMS smaller than that of NN at the 95% power (upper diagram in Fig. 2).

Fig. 2 shows that the upward and downward bursts of neutron power signals are directly associated with the downward or upward movement of the CPS CR groups 10, 11, and 12. At a low power, in the nighttime period,

XOs are suppressed by the upward movement of the CPS CR groups 10 and 11. These two oppositely directed reactivity effects cause the upward NN bursts to decrease in amplitude, while the NN background RMS remains practically unchanged. Even after the CPS CRs stop moving and, as a result, the XOs are suppressed, NN is a nearly steady-state process up to the time point when the 55%-95% transient begins. Other CRAs, apart from the movement of the CPS CR rods at a power level of 55%, do not change the NN RMS. Therefore, the CPS CR movements, as CRAs, perturb the in-core neutron field heavier than other CRAs. The transition to a power of 95% via the upward movement of the CPS CR group 12 is accompanied not only by a growth in the amplitude of the neutron power bursts but also by a slow growth in the NN RMS.

Any changes in neutron power change the thermal-hydraulic characteristics of the coolant and, specifically, the amount of the vapor phase changes even if obtained as a result of the so-called subcooled boiling<sup>1</sup> of the coolant.

## “Fast” noise measurements at VVER-1200 reactor plants

The vapor phase collapse as a result of the reactor power reduction leads to the positive reactivity release. Therefore, the amount of the coolant vapor phase changes in the course of the maneuvering mode introducing so positive or negative reactivity.

Increasing the amount of the coolant vapor phase makes the neutron energy spectrum (not to be confused with the NN frequency spectrum) harder, i.e. there is a shift towards high energies or towards “fast” neutrons. The properties of a two-phase coolant as the neutron moderator deteriorate, as compared with a single-phase water coolant, i.e. the ratio between “fast” and “slow” neutrons changes in favor of the former. At a low reactor power, the neutron energy spectrum becomes “softer”, followed by a sort of spectral core regulation due to a change in the uranium-water ratio accompanied by a new reactivity source in the XO form, i.e., the nuclide composition of in-core fissile isotopes at different power levels changes with a daily frequency. Eventually, to keep reactivity at a zero level during power operation, the additional reactivity margin can be used which shortens the fuel life. Such effects are monitored with the use of high-frequency neutron-noise measurements.

Noise analysis was used earlier only for steady-state time series, which corresponds to the steady state of the reactor plant. A maneuvering mode will obviously lead to the neutron field unsteadiness. It can be analyzed together in both the time and frequency domains taking into account the type of unsteadiness. One way for the spectral analysis of unsteady time series is to assume that the unsteadiness is “slow”.

<sup>1</sup> By “subcooled boiling” the authors mean the type of boiling that occurs when a liquid with a temperature below the saturation point comes into contact with the heater surface hot enough to cause boiling. In this case, once in contact with the cold liquid, the vapor bubbles condense and there is no resultant removal (accumulation) of the vapor phase into the liquid volume or into the flow core.

The whole of the time realization under investigation is sectioned then into adjacent time segments, each of which includes spectral estimates assuming that the time series is practically steady in each such segment. All spectral response estimates of the same name, obtained in different time segments, are represented in a three-dimensional form with the time axis added and with the so-called spectral waterfall obtained. Fig. 3 shows the DCD waterfalls for two assemblies of neutron measurement channels (NMCs).

We shall consider the novelty the neutron-noise spectral analysis of the maneuvering mode brings about.

The length of one time series segment shall be sufficient to reliably estimate the spectral response. As shown by experience in Arkadov et al. 2018, 2021, the smallest sufficient length is 10 minutes with a sampling frequency of 100 Hz for the neutron noise frequency range of 1 Hz and higher.

If we take into account that the maneuvering mode is recorded for many hours, we obtain a sufficiently large number of spectral estimates for the spectral waterfall. In the 510 minute maneuvering mode under consideration, in particular, we will have a spectral waterfall containing 51 spectral characteristics.

There are two resonant features of the VVER-1200 neutron noise, one of these being the presence of the first vessel acoustic standing wave ( $ASW_{IV}$ ) (Arkadov et al. 2018, 2021) at a frequency of 8.7 Hz under rated conditions (see Fig. 3) which affects all direct-charge detector (DCD) signals and all IC signals. The second resonant feature is a local vibration resonance at 6.1 Hz recorded in the lower DCD1 and DCD2 signals (see Fig. 3), that is, the resonances have different physical origin, different spatial distribution, and different response to the reactor power change. During a single 1 second long CPS CR step, these two resonances are affected by the so-called finite (finitely long) external force resonances: one with a duration of 8 periods, and the other with a duration of 6 periods.

Fig. 3 shows spectral waterfalls for signals of two neutron measurement channels (NMCs) diametrically distant from each other inside the core with coordinates 02-23 and 14-37. We shall consider in detail how the maneuvering mode affects these two spectral features of neutron noise.

Fig. 3 shows that one CPS CR step (CPS CR groups 10, 11, or 12) with a length of exactly 1 second contains a “comb” of integer harmonics of 1 Hz, 2 Hz, 3 Hz, and further up to 10 Hz. These harmonics are low-voltage, just as low-voltage is  $ASW_{IV}$  as such at a frequency of 8.7 Hz. The vibration resonance at a frequency of 6.1 Hz, though having a high Q factor, is however also covered by the 6.0 Hz harmonic with a low Q factor, that is, the “comb” covers both the  $ASW_{IV}$  frequency and the vibration resonance. Resonant excitation is possible.

With the rapid transition from 95% (steady state) to 55% of reactor power via the consecutive downward movement of three CPS CR groups, the whole of the core is affected heavily by multiple equidistant harmonics (those having an equally long 1 Hz spacing between each other). At the same time, the central frequency of  $ASW_{IV}$

at a power of 55% increases as the core average coolant temperature decreases. Throughout the nighttime period with power kept at a level of 55%, the CPS CR group 12 is in the inserted state in the 50% position, and group 11 is not more than in the 62% position. Such deep CPS CR insertion into the core eliminates the point global component of neutron noise in the upper half of the core and results in zero coherences of IC-IC signals in a range of 2 Hz to the  $ASW_{IV}$  frequency (see Fig. 3). When the CPS CRs in groups 10 and 11 moved upward at a power of 55% for the XO suppression, the “comb” amplitude decreased greatly due to the counteraction of two reactivity effects.

The modulations of the core neutron field on the  $ASW_{IV}$  side are barometric due to the reactivity change as a result of the pressure change in the main circulation circuit and are most pronounced where there is no counteraction on the part of the CPS CR absorber rods, i.e. in the lower half of the core, as it can be seen from the DCD signals within the horizon of the third DCD3 and below (see Fig. 3). Within the upper DCD horizons (above DCD3), there is no  $ASW_{IV}$  effect with the CPS CRs inserted into the core to a level of 50% (half of the core). In the upper half of the core, the CPS CRs absorb all neutron effects in excess of 3 Hz. The ionization chamber “integrates” large core volumes, so  $ASW_{IV}$  is still a global effect in the coherences of IC-IC signals but with a smaller amplitude. The frequency of the vibration resonance (6.1 Hz) does not depend on the reactor power level (unlike the  $ASW_{IV}$  frequency), while its amplitude increased slightly in the 55%-95% transient (see Fig. 3) due to the vibration resonance being localized in the lower part of the core where the CPS CR impact is much smaller than in the upper half of the core.

The autospectral power densities (ASPD) of the same-named DCD signals from two distant NMCs (see Fig. 3) practically follow each other. Within the DCD7 horizon, the “comb” assumes the maximum amplitudes unlike the DCD3 horizon, and the perturbation from the CPS CR movement is as small as it can be for the lower DCD1 and DCD2 horizons. At a power of 55%, when the CPS CRs are in the upper half of the core, the NN power in the DCD7 horizon is negligibly small.  $ASW_{IV}$  manifests itself only at a power of 95% and within the DCD3 horizon and below.

To correlate the ASPD amplitudes of the IC1 signal in different states of a maneuvering mode, all ASPD estimates (51 functions), collected into three groups, are presented in a traditional form in Fig. 4. All three families are presented in the same dynamic range ( $Y$  axis). Group 1 contains ASPDs at a power of 95% and in the 95%-55% transient (four functions altogether), group 2 contains ASPDs only at a power of 55%, and group 3 contains ASPDs in the 55%-95% transient and at a power of 95%. It can be seen in group 1 that there is a major perturbation caused by the CPS CR movement (the scale of the ASPD presentation is logarithmic) and that it is periodic in frequency, which is hard to detect in the time domain. The “comb” starts at 4 Hz and extends to 11 Hz with a step of 1 Hz.

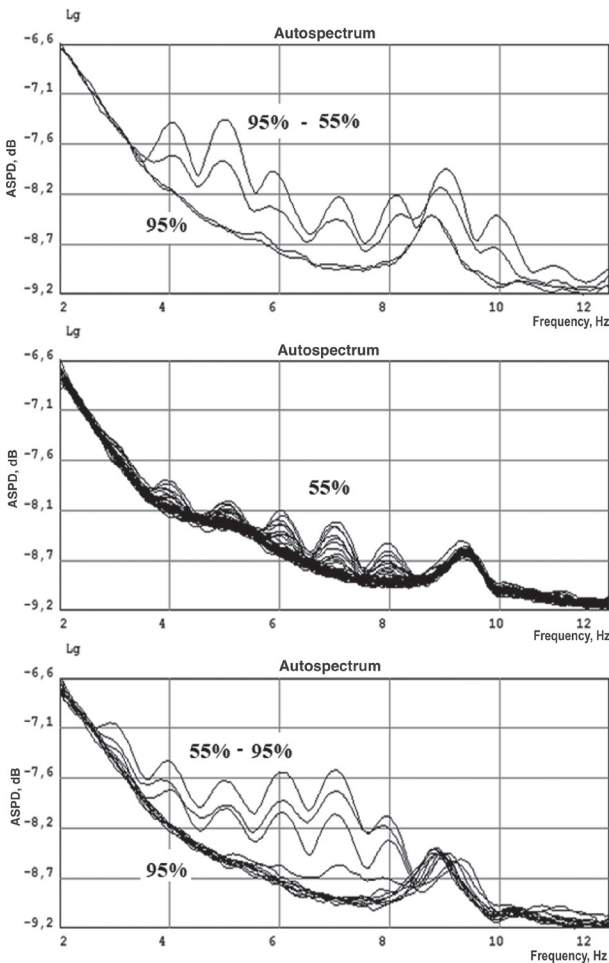


**Figure 4.** Fragments of neutron power as shown by IC signals at the beginning of the power reduction due to the downward CPS CR movement in the 95–55% transient (upper diagram), steady state (middle diagram), and at the beginning of the power increase in the 55–95% transient due to the upward movement of group 12 (lower diagram).

Besides, one can see how the  $ASW_{IV}$  amplitude and frequency increased. In group 2, there is an ASPD “comb,” which is relatively stable and has a much smaller amplitude due to the upward movement of two CPS CR groups in the course of the XO suppression.

In group 3 again, there is an increase in the ASPD amplitude with the upward movement of the CPS CR group 12. The “comb” starts at 3 Hz this time and, by capturing  $ASW_{IV}$ , decreases its frequency. Changes in the  $ASW_{IV}$  frequency and amplitude are observed only when the CPS CRs are in motion, i.e. there is no continuous trend of these parameters that shall accompany the resonance excitation.

## Vertical correlations

In addition to the DCD signal ASPDs (see Fig. 3), the coherence functions of DCD-DCD signals also make it possible to determine the spatial dependences of the in-core neutron-noise effects. Adjacent DCDs of one NMC

or DCDs of two neighboring NMC1 and NMC2 reveal, among other things, local NN effects. DCDs of different NMCs, diametrically distant inside the core, reveal global NN effects.

The coherence functions of the signals from adjacent lower DCDs of one NMC (DCD21-DCD22) (Fig. 5) do not practically respond to the reactor power change, that is, there is no “comb” of resonances with a step of 1 Hz. These are dominated by correlations for the global (point) neutron-noise component of up to 3 Hz and the vibration resonance of 6.1 Hz. As the 55–95% transient starts, when the CPS CR group 12 begins to move upward, there is an increase in the 6.1 Hz vibration resonance amplitude in just one coherence function. This is the resonant effect of the CPS control rods on the FA vibrations which is not continued.

The coherence functions of nearby signals but from upper DCDs of one NMC (DCD26-DCD27) (see Fig. 3) show a strong dependence on both downward and upward movements of all three CPS CR groups. Within the core horizons where the CPS CR absorber rods move (in the 95–55% and 55–95% transients), there is a frequency “comb” observed. At a power level of 55%, when the CPS CRs are in the upper half of the core, only correlations for the global (point) neutron-noise component of up to 3 Hz dominate. It is only after the 55–95% transient ends, when the CPS control rods are withdrawn, that the  $ASW_{IV}$  resonance occurs.

The coherence functions of signals from the distant lower DCD11-DCD21 (see Fig. 5) are sensitive only to global neutron effects. On the other hand, they are similar to the coherence functions of signals from adjacent DCD21-DCD22 of one NMC2, which are sensitive to both global and local neutron effects. Then, the vibration resonance at a frequency of 6.1 Hz shall be declared a global phenomenon with the only reservation that this phenomenon propagates only within the lower DCD1 and DCD2 horizons. No vibrations at a frequency of 6.1 Hz are observed above the DCD2 horizon.

The nighttime reactor mode at a power of 55% involved three CPS CR groups having been inserted at once deeply into the core with a high efficiency changing so substantially the distribution of neutron-noise sources. As known by the authors, no such experimental studies into the effect of the CPS CRs on the neutron-noise field inside the core have ever been conducted elsewhere.

At a power of 55%, the upper half of the core, where the CPS CRs in group 12 are permanently in the position at a height of 50%, has no local effects and obeys pointwise global kinetics at up to 3 Hz. The absorber rods for the CPS CRs do not allow any high-frequency neutron-noise processes in excess of 3 Hz. In the upper half of the core, there is no barometric neutron effect from the  $ASW_{IV}$  standing wave as well. With the CPS CRs inserted and retained, the effect from  $ASW_{IV}$  manifests itself in the lower half of the core (Fig. 6). In the upper half of the core,  $ASW_{IV}$  is restored again at a power level of 95% when all CPS CRs are withdrawn.

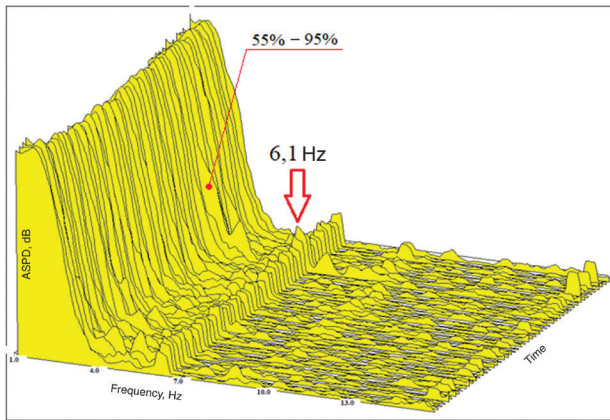


**Figure 5.** Coherence functions for signals from lower DCDs of one NMC (DCD21-DCD22).

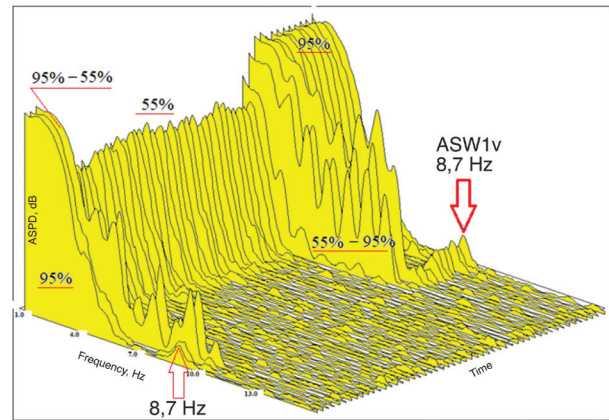


**Figure 6.** Coherence functions of signals from upper DCDs of one NMC (DCD26-DCD27).

## Conclusions

1. After a single step of the CPS CRs, the whole of the core is affected by a practically instantaneous major amplitude impact, which decays for one second if no further CPS CR step takes place within this time. Such fast neutron processes can only be monitored via neutron-noise measurements with an upper frequency of not less 20 Hz.
2. Any changes in neutron power change the thermal-hydraulic characteristics of the coolant and, specifically, the amount of the in-core vapor phase. The properties of a two-phase coolant as the neutron moderator deteriorate, as compared with a single-phase water coolant, i.e. the ratio between “fast” and “slow” neutrons changes in favor of the former. At a low reactor power, the energy spectrum of neutrons becomes “softer”, followed by a sort of in-core spectral regulation due to a change in the uranium-water ratio being accompanied by a new source of reactivity in the form of XOs. The nuclide composition of in-core fissile isotopes at different power levels changes with a daily frequency. Eventually, an additional reactivity margin can be used to

keep reactivity at a zero level during power operation which shortens the fuel life.

3. The neutron detector signal bursts from the CPS control rod movement are high-frequency recurring neutron power forms, which, when in a frequency form, look like a “comb” with a constant step of 1 Hz. A single step of the CPS CRs with a length of exactly 1 second contains a “comb” of integer harmonics of 1 Hz, 2 Hz, 3 Hz, and further up to 10 Hz. With frequently and periodically moving CPS CRs, resonant excitation for representative neutron noise features (vessel standing wave at a frequency of 8.7 Hz and a local vibration resonance of 6.1 Hz) is possible. The danger consists in an abnormal operating mode of automatics when it enters an unsteady self-regulation mode. Control in different dynamic transients shall be simulated in detail to avoid periodic and frequent effects. In the event of a maneuvering mode, the frequency of reactivity introduction from the CPS CR movement needs to be limited.
4. The CPS CRs inserted deeply into the core at a reduced power of 55% absorb all neutron-noise effects in excess of 2 Hz in the upper half of the core.

## References

- Arkadov GV, Pavelko VI, Slepov MT (2018) Vibroacoustics in applications to the VVER-1200 reactor plant. Series: Library of Technical Diagnostics of Nuclear Power Plants. Moscow. Nauka Publisher, 469 pp. [ISBN 978-5-02-040138-9] [in Russian]
- Arkadov GV, Pavelko VI, Slepov MT (2021) Noise monitoring in applications to the VVER-1200 reactor plant. Series: Library of Technical Diagnostics of Nuclear Power Plants. Moscow. Nauka Publisher, 222 pp. [ISBN 978-5-02-040869-2] [in Russian]
- Averyanova SP, Dubov AA, Kosourov KB, Semchenkov YuM, Filimonov PE (2012) VVER-1200/1300 operation in a daily load schedule. Atomic Energy 113: 305–313. <https://doi.org/10.1007/s10512-013-9637-7>
- Averyanova SP, Dubov AA, Kosourov KB, Filimonov PE (2010) Temperature regulation and maneuverability of VVER-1000. Atomic Energy 109: 246–251. <https://doi.org/10.1007/s10512-011-9352-1>
- Averyanova SP, Dubov AA, Kosourov KB, Semchenkov YuM, Filimonov PE (2013) Development of methods for VVER-1200/1300 control in a daily load schedule. Atomic Energy 114: 308–314. <https://doi.org/10.1007/s10512-013-9716-9>
- Averyanova SP, Semchenkov YuM, Filimonov PE, Gorokhov AK, Molchanov VL, Korennoy AA, Makeev VP (2005) Adoption of improved algorithms for controlling the energy release of a VVER-1000 core at the Khmel’nitskii nuclear power plant. Atomic Energy 98(6): 386–393. <https://doi.org/10.1007/s10512-005-0222-6>

- Aver'yanova SP, Lunin GL, Proselkov VN, Filimonov PE, Gorokhov AK, Bogatyr' SM, Medvedev AV, Povarov VP (2002) Using the offset – power diagram to monitor the local linear power density of fuel elements in a VVER-1000 core. *Atomic Energy* 93: 547–553. <https://doi.org/10.1023/A:1020832414569>
- Aver'yanova SP, Kosourov KB, Semchenkov YuM, Filimonov PE, Liu Haitao, Li Iou (2007) Testing of improved algorithms controlling energy release in VVER-1000 in maneuvering regimes at the Tianwan nuclear power plant (China). *Atomic Energy* 103: 836–844. <https://doi.org/10.1007/s10512-007-0133-9>
- Aver'yanova SP, Kovel AI, Mamichev VV, Filimonov PE (2008) Development, introduction, and current state of the computational program “reactor simulator”. *Atomic Energy* 105: 303–307. <https://doi.org/10.1007/s10512-009-9100-y>
- Aver'yanova SP, Filimonov PE (2009) Xenon stability of VVER-1200. *Atomic Energy* 107: 424–428. <https://doi.org/10.1007/s10512-010-9246-7>
- Aver'yanova SP, Vokhmyanina NS, Zlobin DA, Filimonov PE, Kuznetsov VI, Lagovskii VB (2017) Offset-cardinality phase diagram method of controlling reactor power. *Atomic Energy* 121: 155–160. <https://doi.org/10.1007/s10512-017-0176-5>
- Aver'yanova SP, Vokhmyanina NS, Zlobin DA, Filimonov PE, Povarov VP (2018) Investigation of transient xenon processes in VVER-1200 at the novovoronezh NPP. *Atomic Energy* 124: 215–220. <https://doi.org/10.1007/s10512-018-0400-y>
- Dolgoplov NYu, Mezentsev PP (2022) Results of tests of maneuverable modes at NPP power units-2006. Collection of Abstracts of the 6<sup>th</sup> International Scientific and Technical Conference “Commissioning of NPP”. Moscow, Atomtekhenenergo, 11–12. [in Russian]
- Filimonov PE, Semchenkov YuM, Malyshev VV, Dolgoplov NYu, Povarov VP, Gusev IN (2020) VVER-1200 tests in No. 6 unit of the novovoronezh NPP during operation in a daily load schedule. *Atomic Energy* 129: 113–121. <https://doi.org/10.1007/s10512-021-00721-y>
- Filimonov PE, Dubov AA, Semchenkov YuM, Bondar AM, Vorobyev DF (2022) Testing of nonstationary VVER-1200 operating regimes in belarusian NPP No. 1. *Atomic Energy* 131: 241–248. <https://doi.org/10.1007/s10512-022-00873-5>
- Glushenkov RS (2015) The study of key aspects of the introduction of the regime of daily power regulation at the NPP of Ukraine. *Technological Audit and Production Reserves* 2(1(22)): 18–26. <https://doi.org/10.15587/2312-8372.2015.41404> [in Russian]
- Ignatenko EI, Pytkin YuN (1985) Maneuverability of VVER Type Reactors. Library of the Operator of the NPP. Issue 6. Moscow. Energoatomizdat, 88 pp. [in Russian]
- Povarov VP, Ukraintsev VF, Golubev EI, Zhuk MM (2021) Experimental Studies of Neutron-Physical Processes in the VVER-1200 Core. Novovoronezh, 264 pp. [ISBN978-5-6046275-0-1][in Russian]
- Tereshonok VA, Stepanov VS, Povarov VP, Lebedev OV, Makeev VV (2003) Prevention and suppression of axial xenon oscillations in the VVER-1000 core. *Thermal Engineering* 5: 11–15. [https://elibrary.ru/download/elibrary\\_18806680\\_94837472.pdf](https://elibrary.ru/download/elibrary_18806680_94837472.pdf) [accessed Aug. 04, 2023] [in Russian]
- Vygovsky SB, Al Malkawi RT, Khachatryan AG, Abrahamyan SA (2018) Optimization of control algorithms for nuclear power plants with VVER-1200 to minimize water exchange in the 1<sup>st</sup> circuit during the implementation of daily maneuvering modes. *Global Nuclear Safety* 28: 49–63. <https://doi.org/10.26583/gns-2018-03-07> [in Russian]